Modelling Mechanics of Fibre Network using Discrete Element Method

Per Bergström

Main supervisor: Tetsu Uesaka
Co-supervisors: Charlotta Hanson, Kaarlo Niskanen

Faculty of Science, Technology and Media
Thesis for Licentiate degree in Chemistry
Mid Sweden University
Sundsvall, 2018-09-17

Akademisk avhandling som med tillstånd av Mittuniversitetet i Sundsvall framläggs till offentlig granskning för avläggande av teknologie licentiatexamen onsdagen den 24e oktober 2018 kl 13:00 i sal O111, Mittuniversitetet Sundsvall. Seminariet kommer att hållas på engelska.

Modelling Mechanics of Fibre Network using Discrete Element Method

Printed by Mid Sweden University, Sundsvall
ISSN: 1652-8948
ISBN: 978-91-88527-64-6

Faculty of Science, Technology and Media
Mid Sweden University, SE-851 70 Sundsvall, Sweden
Phone: +46 (0)10 142 80 00
Mid Sweden University Licentiate Thesis 144

Table of Contents

Abstract

Low-density fibre networks are a fundamental structural framework of everyday hygiene products, such as baby diapers, incontinence and feminine care products, bathroom tissue and kitchen towels. These networks are a random assembly of fibres, loosely bonded and oriented in the plane direction.

Designing such a complex network structure for better performance, better use of materials and lower cost is a constant challenge for product designers, requiring in-depth knowledge and understanding of the structure and properties on the particle (fibre) level.

This thesis concerns the development of a computational design platform that will generate low-density fibre networks and test their properties, seamlessly, with the aim to deepening the fundamental understanding of the micromechanics of this class of fibre networks.

To achieve this goal, we have used a particle-based method, the Discrete Element Method (DEM), to model the fibres and fibre networks. A fibre is modelled as a series of linked beads, so that one can consider both its axial properties (stretching and bending) and transverse properties (shearing, twisting and transverse compression). For manufacturing simulations, we developed the models for depositing fibres to form a fibre network, consolidating the fibre network, compressing to make a 3D-structured network, and creating creping. For testing the end-use performance, we have developed two models and investigated the micromechanics of the fibre network in uniaxial compression in the thickness direction (ZD) and in uniaxial tension in the in-plane direction.

In the ZD-uniaxial compression of entangled (unbonded) fibre networks, the compression stress exhibits a power-law relationship with density, with a threshold density. During compression, the fibre deformation mode changed from fibre bending to the transverse compression of fibre. Accordingly, the transverse properties of the fibres had a large impact on the constitutive relation. By considering a realistic value for the transverse fibre property, we were able to predict the values of the exponent widely observed in the experimental literature. We have found that the deviation of the experimental values from those predictions by the earlier theoretical studies is due to the neglect of the transverse fibre property.

For tensile properties of bonded networks, we have investigated scaling of network strength with density and fibre–fibre bond strength. The network strength showed beautiful scaling behaviour with both density and bond strength, with exponents 1.88 and 1.08 respectively. The elastic modulus of the network, on the other hand, showed a changing exponent (from 2.16 to 1.69) with density in accordance with previous results in the literature. We have also reconfirmed that, with increasing density, the deformation mode changes from bending to stretching. The predicted results for both elastic modulus and strength agreed very well with experimental data of fibre networks of varying densities reported in the literature.

We have developed a computational platform, based on DEM, for accurately modelling a fibre network from its manufacturing process to product properties. This is a tool that allows a versatile design of materials and products used for hygiene products, providing a promising venue for exploring the parameter space of new material and process design.

Svensk sammanfattning

Fibernätverk med låg densitet är en vanligt förekommande struktur för vardagliga hygienprodukter, såsom blöjor, inkontinens och femininvårdsprodukter, pappershanddukar och kökspapper. Dessa nätverk består av en slumpmässig sammansättning av fibrer, löst bundna och orienterade i planriktningen.

Att utforma en sådan komplex nätverksstruktur för bättre prestanda, bättre användning av material och lägre kostnad är en ständig utmaning för produktdesigners, vilket kräver djup kunskap och förståelse för strukturen och egenskaperna på partikelns (fiber) nivå. Denna avhandling handlar om utveckling av en beräkningsmodellplattform som kommer att skapa fibernätverk med låg densitet och testa mekaniska egenskaper sömlöst med sikte på att fördjupa den grundläggande förståelsen för mikromekaniken i denna klass av fibernätverk.

För att uppnå detta mål har vi använt en partikelbaserad metod, Discrete Element Method (DEM), för att modellera fibrerna och fibernätverket. En fiber är modellerad som en serie länkade pärlor, så att man kan beakta både dess axiella egenskaper (sträckning och böjning) och tvärgående egenskaper (skjuvning, vridning och tvärgående kompression). För tillverkningssimuleringar utvecklade vi modellerna för deponering av fibrer för att bilda ett fibernätverk, konsolidera fibernätverket, komprimera för att skapa ett 3D-strukturerat nätverk och skapa crepning. För att testa slutanvändningsprestandan har vi utvecklat två modeller och undersökt fibernätverkets mikromekanik i enaxlig kompression i tjockleksriktningen (ZD) och i enaxlig spänning i planriktningen.

I den ZD-enaxliga komprimeringen av intrasslade (obundna) fibernätverk uppvisar kompressionsspänningen ett potenslagsförhållande med densitet, med en tröskeldensitet. Under kompressionen ändrades fiberdeformationsmoden från fiberböjning till tvärgående kompression av fibern. Följaktligen hade fibrernas tvärgående egenskaper en stor inverkan på det konstitutiva förhållandet. Genom att ta hänsyn till ett realistiskt värde för tvärgående fiberegenskaper, kunde vi förutse värden för exponenten som observerats i experimentell litteratur. Vi har funnit att avvikelsen från experimentella värden för förutsägelser enligt de tidigare teoretiska studierna beror på försummelsen av tvärgående fiberegenskaper.

För dragegenskaper hos bundna nätverk har vi undersökt en skalning av nätverksstyrka med densitet- och fiber-fiber bindningsstyrka.

Nätverksstyrkan visade god överenstämmelse i skalningsbeteende med både densitet och bindningsstyrka, med exponenterna 1,88 respektive 1,08. Elasticitetsmodulen i nätverket visade å andra sidan en skiftande exponent (från 2,16 till 1,69) med densitet i enlighet med tidigare resultat i litteraturen. Vi har också bekräftat att, med ökad densitet, förändras deformationsmoden från böjning till sträckning. De förutsagda resultaten för både elasticitetsmodul och styrka överensstämde mycket bra med experimentella data av fibernätverk med varierande densiteter som rapporterats i litteraturen.

Vi har utvecklat en beräkningsplattform baserad på DEM för att exakt modellera ett fibernätverk från tillverkningsprocessen till produktegenskaper. Detta är ett verktyg som möjliggör en mångsidig design av material och produkter som används för hygienprodukter, vilket ger en lovande platform för att utforska parameterutrymmet för ny material och processdesign.

Acknowledgements

I would like to gratefully acknowledge the Knowledge Foundation, SCA Forest Products AB, Essity Hygiene and Health AB and Nalco Water, An Eco-lab Company for various support provided for this work, as well as the Swedish National Infrastructure for Computing (SNIC) at HPC2N, which provided resources for performing the simulations. Equal gratitude is given for the dedicated help and support of my supervisor Tetsu Uesaka as well as the unwavering support from my employer Essity, especially from my dear colleague and friend Charlotta Hanson, thank you. I extend thanks to my co-workers at Mid Sweden University, Shakhawath, Amanda and Sohan, for all their help and support. Shakhawath Hossain deserves a special thank you for his contribution to this work, endless discussions and for being a good friend to lift my spirits. Finally, I would like to thank my family – Sofia, Märtha and Abbe – without your love and support none of this would have been possible.

List of papers

Paper I: Computational Design of Fibre Network by Discrete Element Method

Paper II: Uniaxial Compression of Three-Dimensional Entangled Fibre Networks: Impacts of Contact Interactions

Paper III: Scaling Behaviour of Strength of 3D-, Semi-flexible-, Cross-linked Fibre Network

1 Introduction

This thesis concerns modelling of mechanics of fibre networks, especially for a wide range of low-density fibre-based hygiene products, such as baby diapers, incontinence and feminine care products, bathroom tissue and kitchen towels. For these soft products, some of their primary performance properties are very much related to the mechanics of the respective fibre networks. Softness, pliability and structural integrity are some of the most important product properties. These properties are strongly related to the selection of fibres and chemical additives as well as formation and process conditions during production. The production of this range of hygiene products typically consists of fibre networks being created in either dry-forming or wet-forming processes where fibres are essentially laid down on a perforated surface such as wires. The network may thereafter be subjected to additional mechanical production steps such as different types of compression, embossing, creping, etc. in order to achieve the desired product properties.

The importance of mechanical properties, both in production and in end-use, poses constant challenges for product designers in designing the network structure for better performance, better use of materials, and lower cost. These challenges demand ever-increasing need for in-depth knowledge and understanding of the structure and properties on the particle (fibre) level. In using a modelling approach to create this in-depth knowledge and understanding, the choice of the models, both for attaining a representative network structure and resolving network deformation, is crucial for the end result. From an application point of view, a key question is resolving the dependence of mechanical properties on individual components, i.e. fibres, and their properties. The reason for this is that a typical design question is not about constitutive parameters but rather about the effects of fibre properties, such as fibre shape, fibre length and fibre stiffness, on end-use performance. Another important question is how specific steps of the manufacturing process, such as compression, creping, embossing, etc., influence network structures, such as local uniformity of fibre distributions, inhomogeneity and fibre orientation. This brings a need for seamlessly connecting modelling of these production steps with modelling of performance.

In this study we choose the approach of modelling the network as a discrete system in 3D and resolve individual fibre–fibre interactions to evaluate network deformations. The method we have used is a particle-based method called the Discrete Element Method, or DEM, which is a robust and intuitive method well suited for handling important features of network deformation such as large deformation, translation/rotation of components, emergence/breakage of contacts between components and network fracture. Using DEM, we have developed a computational platform for designing fibre networks, and investigated two of the most common end-use properties, ZD compression and in-plane tensile properties. In the following, we will review some of the backgrounds of these subjects in the literature.

2 Background

The main function of DEM is to solve the equations of motion (linear momentum conservation and angular momentum conservation) for all interacting particles. This computational method originated from the field of granular flow, such as for sand, grain, snow and powder (Cundall & Strack, 1979). Although modelling the system is rather straightforward and intuitive, the computational demand is heavy, as it is for molecular dynamic methods, and, therefore, earlier models are rather limited in terms of the system size and the types of interaction parameters considered. However, as is known, ever-increasing computer power and further development of essential algorithms, such as contact search and time integration, e.g. (Williams & O'Connor, 1999), (Zhu, Zhou, Yang, & Yu, 2008), (Munjiza, 2004), (Welling & Germano, 2011), have led to DEM becoming a more and more viable option today for analysing the problems of complex material behaviour and nonlinear dynamics.

Modelling of fibre network compressibility has a long history, originating in the textile area. Here, "compressibility" is defined as the uniaxial compression response of fibre network in the thickness direction (ZD). The pioneering work of compression modelling is the semi-empirical model developed by van Wyk (van Wyk, 1946) where he proposed the expression for pressure, P, as a function of fibre volume fraction, ϕ:

$$P \propto ((\frac{\phi}{\phi_0})^n - 1)$$

where ϕ_0 is the initial volume fraction and the exponent n is used to characterize development of pressure and is found by van Wyk to be equal to 3 for initially isotropic fibre networks. This work has subsequently been followed up by many researchers in statistical geometry and micromechanics of fibre networks (Carnaby & Pan, 1989), (Pan, 1993), (Lee & Carnaby, 1992), (Lee & Lee, 1985), (Komori, Itoh, & Takaku, 1992), (Komori & Makishima, 1977), (Komori & Itoh, 1994), (Toll, 1998), (Toll & Månson, 1995). These studies addressed the effects of non-straight fibres, anisotropy, the number of fibre–fibre contacts and the steric hindrance effect on fibre–fibre contacts in 3D. Notably it was shown that the exponent n becomes equal to 5 for networks with planar fibre orientation (Toll & Månson, 1995), which is in contrast to 3 for an isotropic fibre network, as obtained by van Wyk. However, the analytical models developed require some crucial assumptions, such as affine deformation of a fibre beam segment or the assumption of uniform force-increment to the contact points. The models also assume bending deformation of fibres as the only fibre deformation mode, ignoring fibre shear, twist, stretch and deformation of fibre in the transverse direction. Friction and sliding between fibres is also not explicitly considered.

The limitations to the earlier models have been addressed by researchers developing numerical models. (Beil & Roberts, 2002), (Barbier, Dendievel, & Rodney, 2009), (Rodney, Fivel, & Dendievel, 2005), (Durville, 2005), (Subramanian & Picu, 2011), (Abd El-Rahman & Tucker III, 2013). The numerical models could account for fibre sliding and were able to reproduce some hysteresis response and the irreversible deformation due to fibre rearrangement. The fibre deformation mechanism has also been further clarified, where in the initial stage of compression fibres deform mainly in the bending mode, whereas in the high-density range the fibre axial deformation mode starts to dominate (Subramanian & Picu, 2011). However, the compression behaviour near the initial density and response in the volume fraction approaching 1 are still very difficult to determine accurately even with these numerical models.

An important point regarding the deformation mechanism remains – the numerical results were obtained for isotropic networks subjected to triaxial compression as opposed to networks with more planar fibre orientation subjected to the uniaxial compression commonly found for fibre-based hygiene products.

Tensile properties of networks is another area with great implications for both product performance and production of this class of hygiene products. Similar to the modelling of compression, the most classic works are the models developed by Cox (Cox, 1952). He considered two cases: one when fibres are assumed to undergo affine deformation (very long fibre or high-density sheets), and the other a finite fibre length effect (called shear-lag effect). Cox's work has provided the important foundation for subsequent researchers. As the models by Cox were intended for paper-like, relatively high-density networks, he considered only axial stiffness of fibres. Subsequent work tried to incorporate more realistic fibre deformation modes to the network model, such as shear and bending (Campbell, 1963), (Van den Akker, 1962), (Kallmes, Stockel, & Bernier, 1963), (Kallmes & Perez, 1965), (Page, Seth, & De Grace, 1979) (Qi, 1997), but still based on either the affine deformation assumption on the contact points or the shear-lag approach. Numerical models for paper networks were developed later over the years and a good review of models for paper fibre networks is available in the literature (Heyden, 2000). The numerical models managed to eliminate the affine or shear-lag assumptions, and also incorporate more realistic features of paper networks, such as fibre orientations, 3D-structures, shear/bending deformations of fibre, finite fibre–fibre bond stiffness, the variabilities of fibre properties and geometries, failure criteria of fibre–fibre bonds, nonlinear stress–strain response of fibres, and fibre–fibre sliding (Yang, 1975), (Rigdahl, Westerlind, & Hollmark, 1984), (Hamlen, 1991), (Åström & Niskanen, 1991) (Åström & Niskanen, 1993) (Åström, Saarinen, Niskanen, & Kurkijrvi, 1994), (Jangmalm, 1996), (Räisänen, Alava, Nieminen, & Niskanen, 1996), (Heyden, 2000), (Borodulina, Kulachenko, Galland, & Nygårds, 2012), (Kulachenko & Uesaka, 2012), (Persson & Isaksson, 2014).

Both tensile properties and ZD-compression properties are known to be very strongly influenced by the density of the fibre network. For tensile properties the effect of network density has been studied extensively by researchers in the physics communities concerning problems in fibre networks for biological systems. Extensive reviews of mechanics of fibre networks are available (Broedersz & MacKintosh, 2014), (Picu, 2011). Network stiffness as a function of density has been studied for isotropic networks in 2D and 3D consisting of one dimensional fibres with axial and bending stiffnesses (Head, Levine, & MacKintosh, 2003), (Wilhelm & Frey, 2003) (Ban, Barocas, Shephard, & Picu, 2016), (Broedersz, Sheinman, & MacKintosh, 2012), (Licup, Sharma, & MacKintosh, 2016). The most important finding (Head, Levine, & MacKintosh, 2003), (Licup, Sharma, & MacKintosh, 2016) is that the system undergoes a crossover between two distinct deformation regimes with increasing density, where in the low-density range the deformation is highly non-affine and dominated by fibre bending, while in the high-density range on the other hand, the deformation is affine and dominated by stretching. This change in regimes leads to a change in scaling of network stiffness where shear modulus G scales as $G \sim \rho^n$ with different exponent n values in the two regimes. In the affine regime, $n = 1$, i.e., the elastic modulus is proportional to density, whereas in the non-affine regime, $n = 2$. An interesting question remains, relevant for the aforementioned range of products – that of whether the elastic modulus of 3D deposited planar fibre networks scales with density in the same way as isotropic 2D and 3D fibre network models in the literature. Second, unlike elastic modulus, there are very few studies on network strength for low-density networks and the question of the scaling behaviour of strength and strain-to-failure with density and fibre–fibre bond strength still remains.

3 Aim

The overall goal of this thesis is to develop fundamental understandings of the complex mechanics of low-density fibre networks in hygiene and paper products. To achieve this, first, a computational design platform has been developed for seamlessly generating and testing fibre networks by using the Discrete Element Method. Second, this new computational tool has been applied to clarify the basic mechanism of ZD-compression and in-plane tensile behaviour of fibre networks.

4 Development of computational design platform for fibre networks

4.1 Modelling fibres

The fundamental element used in DEM is a particle and the underlying principle is particles interacting with each other. These interactions can take various forms, such as contact interactions in the normal direction (compressibility of particles) and tangential direction (friction between particles). Particles may also be bonded together to form structures, such as fibres, interacting with each other through linear or nonlinear forces or torques. The law governing this system of particles is the conservation of linear momentum and angular momentum:

$$m_i \ddot{\boldsymbol{r}}_i = \sum_j \boldsymbol{F}_{ij} + \boldsymbol{F}_i^b \qquad [1]$$

$$\frac{\partial}{\partial t}(\boldsymbol{I}_i \cdot \boldsymbol{\omega}_i) = \sum_j \boldsymbol{T}_{ij} + \boldsymbol{T}_i^b \qquad [2]$$

where m_i is the mass and $\boldsymbol{r}_i$ is the position vector of the i-th particle, $\boldsymbol{F}_{ij}$ is the interaction force between the i-th and j-th particles and $\boldsymbol{F}_i^b$ is the body force acting on the i-th particle. For angular momentum, $\boldsymbol{I}_i$ is the moment of inertia tensor, $\boldsymbol{\omega}_i$ is the angular velocity, $\boldsymbol{T}_{ij}$ is the interaction torque between the i-th and j-th particles and $\boldsymbol{T}_i^b$ is the body torque acting on the i-th particle.

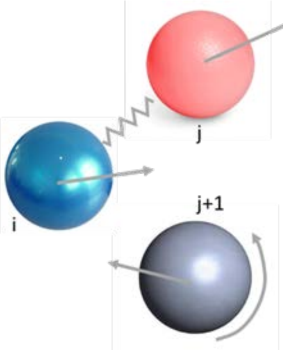

Figure 1: Illustration of particle interactions in DEM. All particles can translate position and rotate around their centre of mass. In this example, particles *i* and *j* are linked by a spring. Particle *j+1* is not linked and can collide with the other particles causing contact forces in the normal and tangential (friction) direction.

The equations for conservation of linear momentum and angular momentum are solved by time integration through the following process:

1. Apply initial conditions for positions and velocities of particles.
2. Calculate all forces and torques according to particle–particle interaction rules.
3. Calculate accelerations from the forces for each particle.
4. Calculate velocities and positions at the next time step for each particle.
5. Go back to step 2.

There are quite a few open-source codes for DEM available and in this work, we have adapted an open-source code called "ESyS-Particle" (Weatherley, Boros, & Hancock, 2014), (Wang, 2009). An important feature of this code is that it is easy to include bonded particles necessary for representing fibres and it also accounts for large rotation effects of particles to ensure that bending and twisting deformation of fibres are correctly considered. The code uses a Verlet list and linked-cell-neighbour search algorithm and the time integration is made using the symplectic Euler method.

As mentioned above, fibres are represented as a string of interconnected particles. In this way, fibre features and properties can be represented in a good and flexible way. Fibre geometry such as diameter and length can be controlled by the diameter and number of particles used to form a fibre, while fibre curl, kink and twist can be controlled by the relative position between particles in equilibrium.

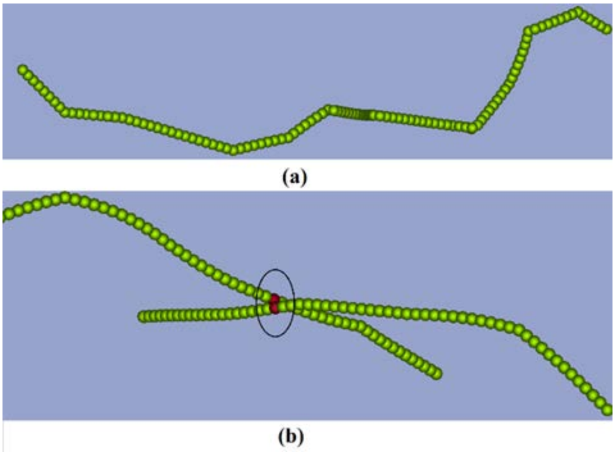

Figure 2: Representation of fibre by particles. (a) Typical fibre consisting of a series of connected particles, and (b) a fibre–fibre bond (or a fibre–fibre contact) as shown by a pair of red particles.

Mechanical properties of the fibres can be modelled by defining appropriate material-specific interactions of the particle–particle bonds within a fibre to represent different fibre deformation modes, such as fibre stiffness in normal, shear bend and twist modes.

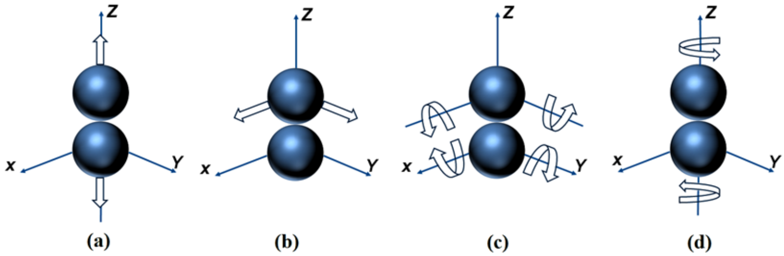

Figure 3: Deformation modes of bonded particles: (a) pure tension or compression, (b) shear in two tangential directions, (c) bending in two directions and (d) twisting. Adapted from (Wang, 2009).

The transverse compressibility of the fibre is defined by setting the particle–particle contact interaction force in the normal direction.

For bonded fibre networks, the representation of mechanical properties of fibre–fibre bonds is defined in the same way as for connected particles within fibres, in the normal, shear, bend, and twist modes. For modelling failures of both fibres and bonds, we use the following empirical failure criterion:

$$\frac{f_r}{F_{r0}} + \frac{|f_s|}{F_{s0}} + \frac{|\tau_b|}{\Gamma_{b0}} + \frac{|\tau_t|}{\Gamma_{t0}} \geq 1$$

where f_r, f_s, τ_b, and τ_t are tensile (compression) force, shear force, bending moment, and twisting moment. The symbols, F_{r0}, F_{s0}, Γ_{b0}, and Γ_{t0} denote their threshold values, respectively.

3.2 Modelling fibre network

Aside from fibre properties, another area of importance is the impact of network properties such as inhomogeneity, fibre orientation, etc., on the mechanics of the network. The network structures studied here are sensitively affected by specific process steps in production. In the case of hygiene products, fibre networks are typically created in either dry-forming or wet-forming processes where fibres are essentially laid down on a perforated surface such as wires. In an attempt to generate more realistic structures relevant to the class of fibre networks seen in hygiene products, we created networks by placing fibres randomly in a 3D space where the dimensions of the space in x and y are used to control sample size and the z-dimension controls the consistency of the fibre suspension. We then proceeded by depositing fibre suspensions using the DEM model under the body forces such as gravity and drag forces.

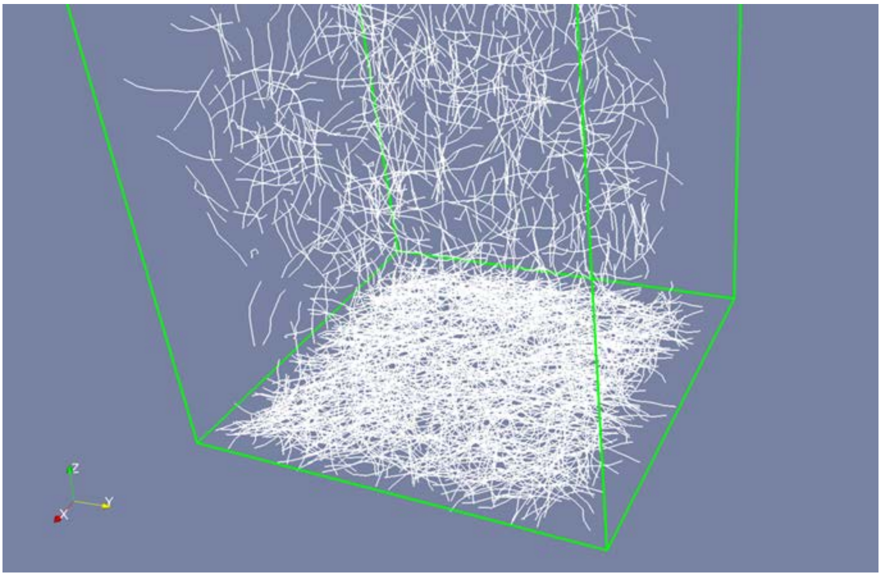

Figure 4: Visualization of the forming of a fibre network by deposition.

After forming, the network of the hygiene product can be subjected to subsequent production steps such as different types of compression or embossing. These processes can readily be modelled using the same DEM model by pressing the surface of the simulated network either with flat or patterned surfaces in order to achieve the desired network.

Bonded fibre–fibre networks can be created at any point in the sequence by defining fibre–fibre "bonds" according to certain criteria (percentage of contacts, contacts with a minimum contact force, etc.).

One basic process in tissue manufacturing which poses an extra level of computational difficulty is the creping process. Simulating a fibre network which has been hit by a blade, e.g. at 2000 m/min, with immediate destruction of 3D microstructures makes DEM ideal for investigating such a highly dynamic and violent process on a microscopic level. In Paper I we presented an example of 3D simulation of creping to create a creped network that can be used to simulate network strength or compressibility.

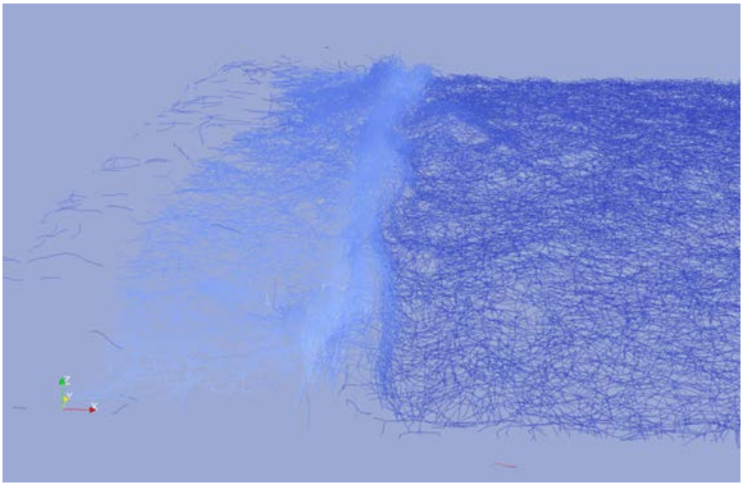

Figure 5: Example of fibre motion in creping process. The colour of fibres represents velocity magnitude (relative to the speed of Yankee dryer). The blue colour represents lower velocity and the white higher velocity. The doctor blade is not shown for the purpose of clarity of fibre motion.

In the resulting network we can see the effect of extensive destruction of the base sheet structure. This includes crepe patterns (frequency and amplitude), the breakage of fibres and fibre–fibre bonds and separation of fibres from the network flying away as fibre dusts.

In the example above, we counted the number of broken bonds within the time period of 0.375 ms, and have found that as many as 30% of the bonds are lost immediately after the explosion.

5 ZD-compression of fibre network

In hygiene products such as diapers and tissue, mechanical responses under uniaxial compression are an integral part of both product properties and production, whether in the form of a baby sitting on a diaper or a compression unit in the production process. Understanding the deformation mechanism and the impact of fibre and network properties, therefore, has a direct impact on product and process development for this class of products. In Paper II, we examined uniaxial compression of unbonded anisotropic fibre networks with fibres oriented mainly in the in-plane direction, with a relatively soft transverse compressibility, a case commonly seen in hygiene products such as diapers and tissue.

Figure 6 shows the components of fibre strain energy stored in the normal (stretching/compression), bending, shearing, twisting and fibre–fibre contact deformation modes during compression.

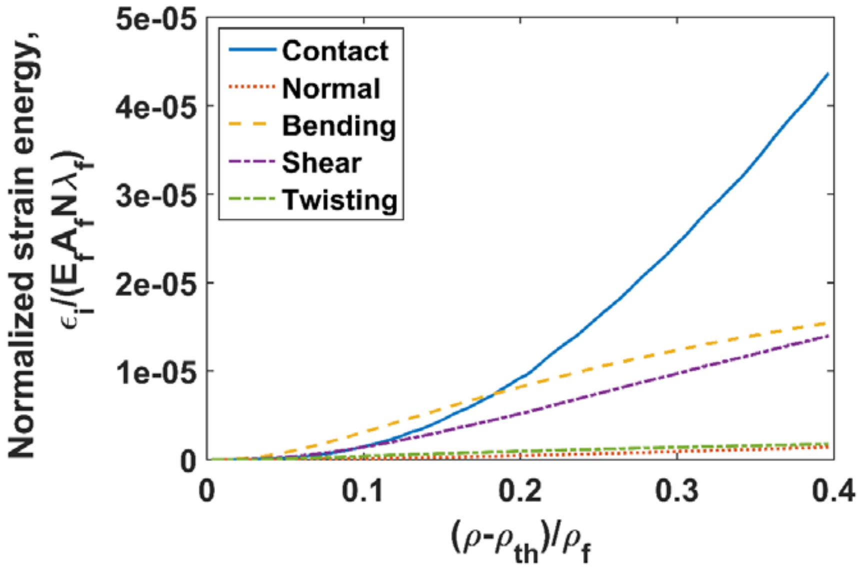

Figure 6: Partition of normalized strain energy, where, ϵ_i represents the strain energy in each deformation mode.

As can be seen in the results, at lower levels of compression bending/shear deformation plays the major role, which is a similar result to previous studies, while at higher levels of compression the fibre–fibre contact energy makes the most significant contribution. This result differs from more frequently studied cases of triaxial compression of initially isotropic networks, where at higher levels of compression the deformation energy in the fibre axial direction takes over (Subramanian & Picu, 2011).

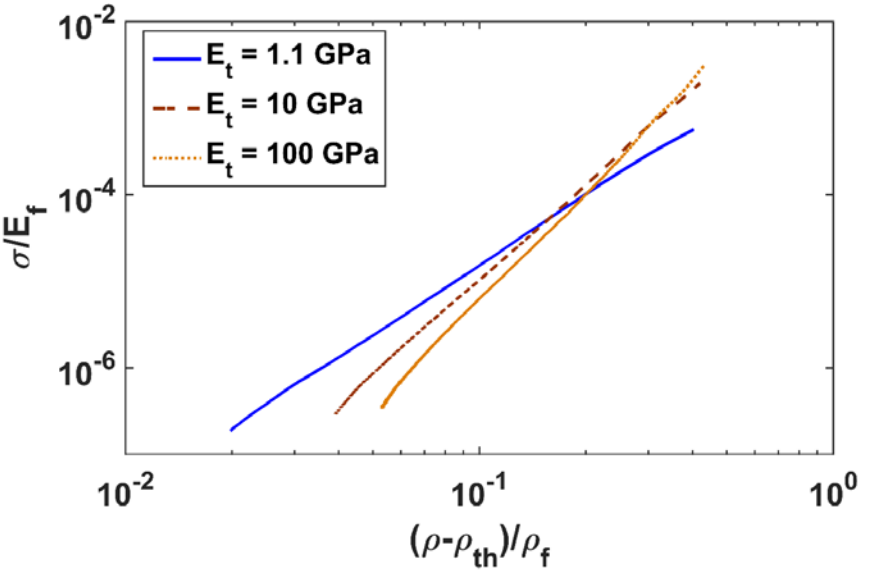

Figure 7: Stress–density relationship (in log-log scale) for different fibre elastic moduli in the transverse direction, E_t

Figure 7 shows a case where the fibre elastic modulus in the transverse direction, E_t, has been increased from 1.1 to 10 and 100 GPa. First, the compression stress shows a power-law dependency on the density with a threshold density for all three simulations. The most notable difference among the three plots is in the exponent (the slope) increasing from 2.67 to 4.1 when increasing the fibre elastic modulus in the transverse direction.

This result is interesting from the point of theoretical predictions by van Wyk (van Wyk, 1946) and Toll (Toll & Månson, 1995); van Wyk predicted the exponent should be 3 for an initially isotropic network, while Toll predicted, for a planar fibre network, the exponent should be 5. Considering the fact that most of the textile and nonwoven fibre networks have more or less planar fibre orientation, then theoretically, the exponent must be more than 3 and approximately 5. However, experimental data routinely exhibited exponent values much less than 3, e.g. (Komori, Itoh, & Takaku, 1992). Figure 7 suggests that the exponent is influenced, not only by fibre orientation, but also by the value of the transverse fibre stiffness.

Even if the fibres are oriented in the in-plane direction, the exponent can be less than 3 for fibres with low transverse stiffness. In the earlier theoretical works, the transverse fibre property was ignored, that is, presuming infinity. Therefore, the exponent was consistently overestimated. Most of the fibres used in textiles and nonwoven fabrics are anisotropic (very high stiffness in the fibre-axis direction and very low stiffness in the transverse direction). Therefore, it is not surprising that the exponent is lower than 3.

Returning to the case with softer transverse contact stiffness of fibres, we further explore the origin of this transition from the bending/shear deformation to fibre–fibre contact (Figure 8).

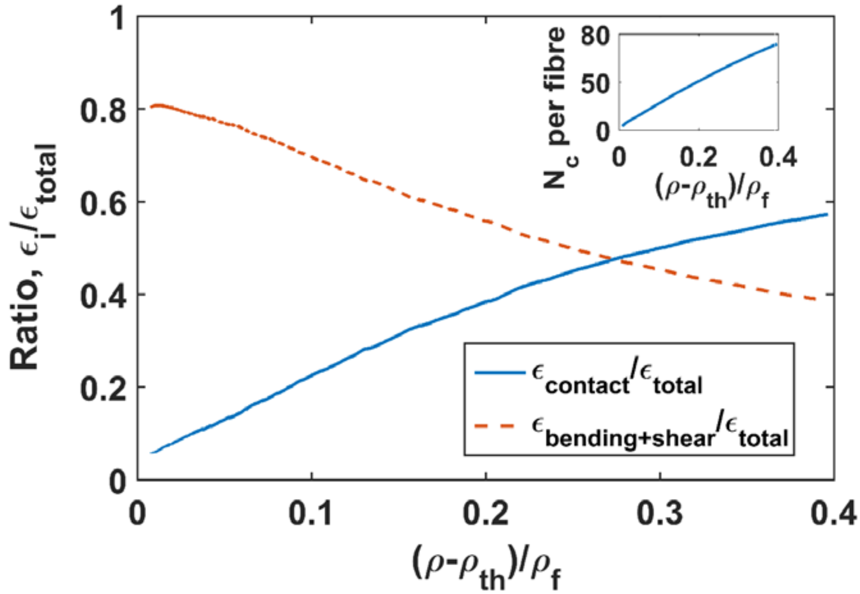

Figure 8: Ratios of strain energy associated with bending and shear modes and fibre–fibre contacts to the total strain energy. (Inset) Number of contacts per fibre is plotted as a function of relative density.

In this case, the transition from the bending/shear deformation to the fibre–fibre contacts happens at a relative density of 0.27. The compression of the network is naturally accompanied by an increase in the number of fibre–fibre contacts per fibre (inset of Figure 8). As the number of contacts increases, clusters of contacts start to form. (A contact cluster is a continuous chain of fibre–fibre contacts defined as a system of N particles, where each particle is in contact with at least one particle from another fibre that belongs to the cluster.) These clusters increase in number and size as compression is increased and in our results some of the large clusters start bridging the top and bottom of the compression surfaces at around the relative density of 0.13. At the maximum compression simulated, about 28% of the clusters are such bridged clusters, carrying 86% of the total contact energy, indicating that such bridged contact clusters are playing a very important role in anisotropic fibre network compression.

To conclude, for ZD-, uniaxial compression of planar fibre networks with realistic transverse properties of fibres studied here, the fibre–fibre contact deformation becomes most significant particularly at a high degree of compression. This is explained by fibres being more oriented in the in-plane direction so that fibre–fibre contacts to a large degree take the uniaxial compression load, especially in the form of contact clusters bridging from top to bottom. Another reason for the dominance of fibre–fibre contact deformation is that, since the realistic transverse fibre property gives soft fibre–fibre contact responses, the deformation of the contact even competes with the lower-energy deformation mode, i.e., bending.

6 In-plane tensile properties of fibre networks

Structural integrity of the network when subjected to tensile load is closely related to both product and production performance in the development of hygiene products such as diapers and tissue, and issues such as web breakage during production or core crumbling of diapers during use are serious concerns in product and process development. In Paper III we investigated network stiffness, strength and strain-to-failure of low-density networks by creating a deposited fibre network consisting of 3D fibres, which is compressed to a range of densities relevant for the types of hygiene products studied in this work.

Looking at the results for network elastic modulus E (Figure 9), assuming $E \propto (\rho - \rho_{th})^n$, we find that the exponent n was not constant but changed slightly from 2.16 to 1.69.

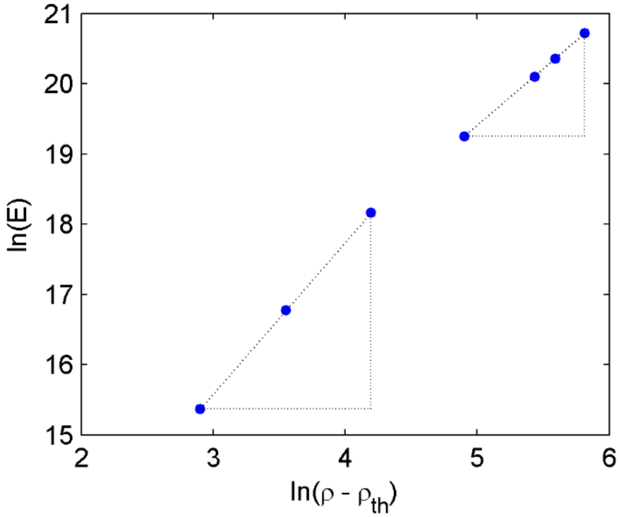

Figure 9: Elastic modulus of network as a function of network density.

The results may correspond with the transition behaviour seen in the literature (Licup, Sharma, & MacKintosh, 2016) with changing values of the exponent from 2 in the lowest density range to 1 in the highest density range. The exponent not reaching 1 in the higher density range could be a steric hinderance effect of the 3D-fibres, i.e., increasing density doesn't necessarily lead to a decrease in the bond-to-bond distance. Further examination of the distribution of total fibre strain energy in the network as a function of density also shows that in the lower density range, most of the strain energy is indeed stored in the fibre bending mode, whereas in the higher density range, it is in the fibre stretching mode (Figure 10). Interestingly, the 3D-fibre effects on mechanical properties (shearing and twisting of fibre) were found to be minimal in tensile deformation. (Note that in the case of ZD-compression, the 3D-fibre effects were very significant, as discussed earlier.)

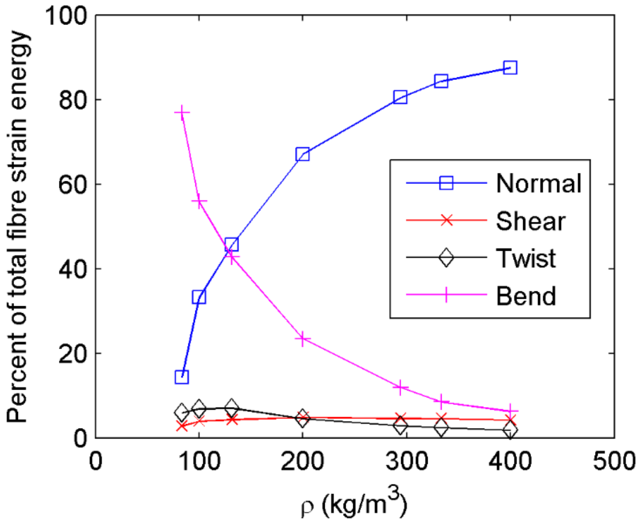

Figure 10: Distribution of total fibre strain energy during deformation for networks with varying density

We proceed to look at the results for network strength as a function of density and bond strength. We varied "bond strength" by multiplying the same factor to all four modes of the bond strength values. The results suggested that the density, $\rho - \rho_{th}$, and shear bond strength, τ_b, are *separable* as variables, and the dependence of network strength, σ_c, is generally expressed as:

$$\sigma_c \propto (\rho - \rho_{th})^m \cdot \tau_b^l$$

All data collapse very nicely as seen in Figure 11, with the exponents $m = 1.88$ and $l = 1.08$.

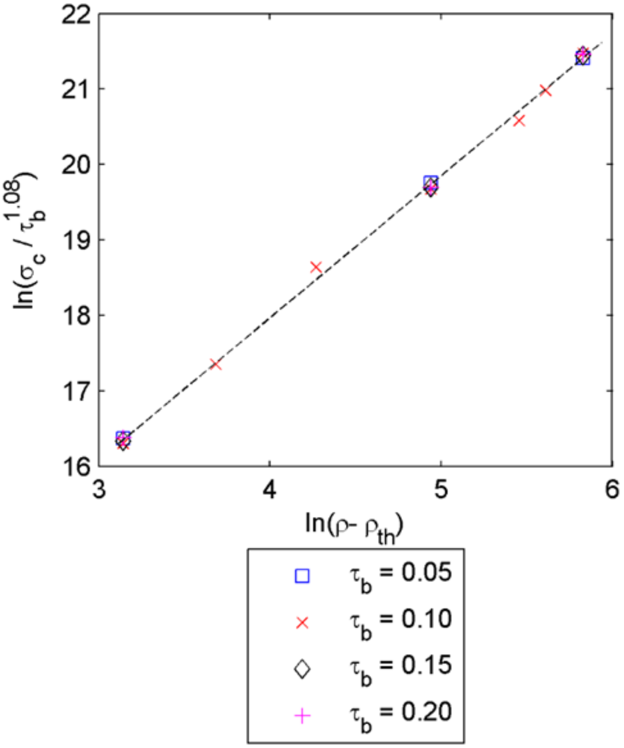

Figure 11: Network strength normalised by bond strength, as a function of network density.

The results show that unlike the elastic modulus there is no obvious inflection in the curve, despite the fact that there is a change in the deformation mode from bending to stretching. This is understandable, because within the density range tested, network failure happened through bond failures, and bond failures in different deformation modes were assumed to occur at the same strain energy in the model.

Next, we look at the network strain-to-failure ε_c in relation to the network density ρ for the simulated networks. Figure 12 shows that ε_c decreases first sharply with density and then gradually increases, forming a unique U-shaped dependence on density. In the same figure, the elastic strain component of the strain-to-failure is also plotted.

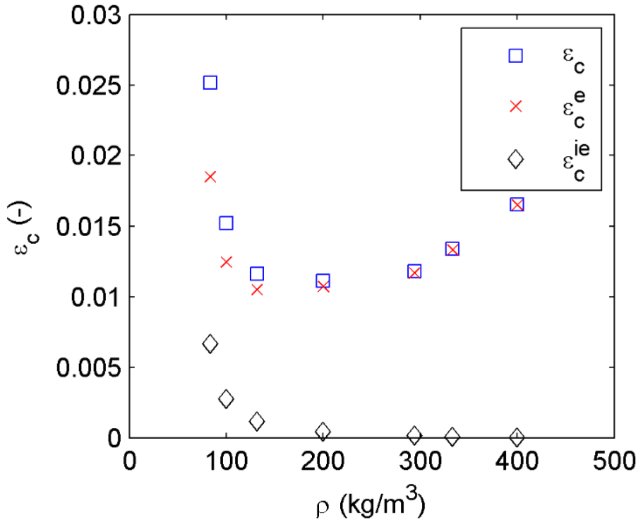

Figure 12: Network strain in terms of total strain, elastic strain and inelastic strain components as a function of density.

The elastic strain component ε_c^e reproduced the U-shaped trend well, particularly in the higher density tange. The U-shape here is due to the fact that, in the low-density range, elastic modulus increases faster than strength with density which is explained by the higher exponent shown above. Since in this system fibres are elastic, the rest of the strain, ε_c^{ie}, is due to breakage of fibre–fibre bonds and we can see how it increases sharply with decreasing density at a very low density range.

These numerical results are quite comparable to those data published in the literature.

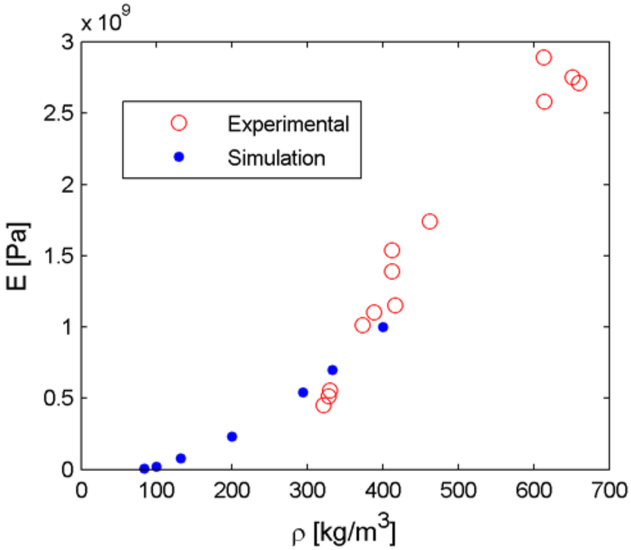

Figure 13: Young's modulus vs density for simulated results compared to experimental data.

Figure 13 shows a comparison with the experimental data (Rigdahl & Hollmark, 1986). The simulated results cover a lower density range of the elastic modulus vs. density curve of typical paper sheets very well.

Figure 14 shows the data of strength vs. density obtained by Eriksson, using hand sheets made of bleached, unbeaten kraft pulp fibres, untreated (Eriksson, Torgnysdotter, & Wågberg, 2006).

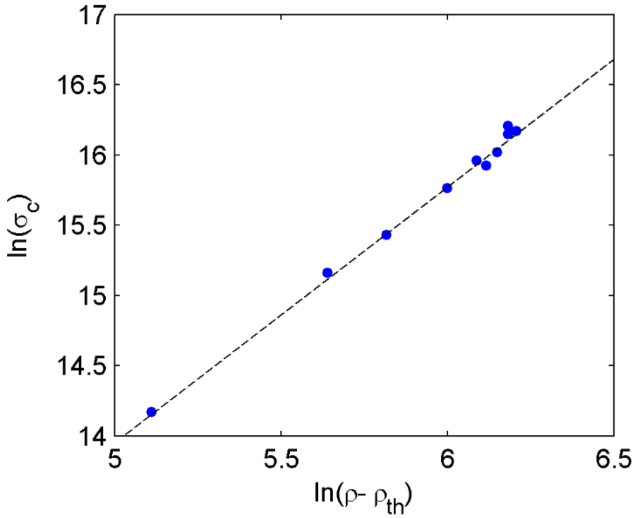

Figure 14: Network strength as a function of density for the data from Eriksson (Eriksson, Torgnysdotter, & Wågberg, 2006)

Fitting the data from Eriksson with a power-law dependence $\sigma_c \propto (\rho - \rho_{th})^m$ with the same threshold density value as the simulation ($\rho_{th} = 63.3\ kg/m^3$), we found the exponent $m = 1.82$. The value showed an excellent agreement with the value of the exponent from the simulation $m = 1.88$.

Finally, we plotted strength vs. strain-to-failure, the so-called "failure envelope", in Figure 15. We find a C-shaped relationship.

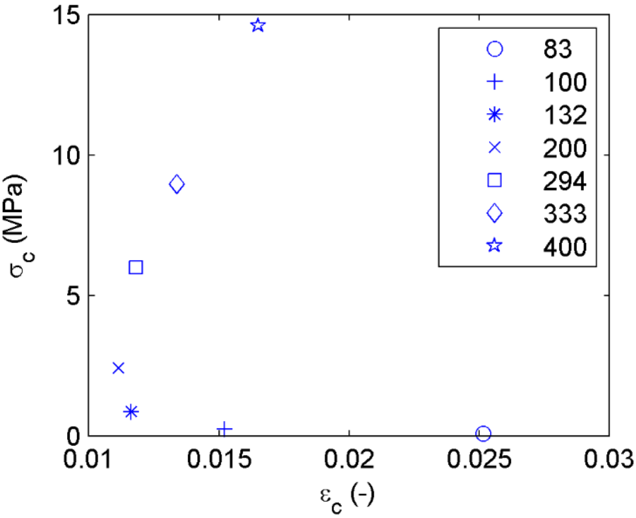

Figure 15: The failure envelope, network strength vs strain at failure, for simulated networks with varying density.

Experimental results from the literature found that the failure envelope of wet web strength of hardwood kraft pulps forms a "C-shape" for wet sheets with varying solid content (i.e., varying degree of bonding) (Gurnagul & Seth, 1997), and we can indeed see that our results also produce a “C-shape” when we vary network density.

In conclusion, the simulation results for elastic modulus, strength and strain-to-failure showed excellent agreements with the respective experimental data in the literature. The scaling result of elastic modulus with density showed, in accordance with previous literature, the typical transition from bending to stretching with changing values of the exponent. Strength, however, showed scaling with density with a constant exponent within the density range investigated. The fact that the numerical results show a constant strength exponent while the deformation mechanism is changing from bending- to stretching-dominated is interesting. It may be explained by the assumption of the fibre–fibre bond breaking criteria in the model, where it is assumed that the fibre–fibre bonds break at the same critical strain energy regardless of the deformation modes. Considering the extremely good agreement with the experimental data, this assumption about bond strength may not be far from reality.

7 Concluding remarks

We have used the Discrete Element Method (DEM) for modelling fibres and fibre network structures, and have solved various problems associated with manufacturing and performance of fibre networks for hygiene products. DEM is a very versatile and intuitive method, and it is ideal for modelling discrete system problems. However, as a numerical method using the explicit scheme, it is very computationally intensive. Particularly for large contact problems, such as the initial state of ZD-compression for high transverse stiffness, and creping simulations, one needs to reduce a time-step to a prohibitively low level and thus carry a huge computational cost. In order to overcome such problems, we need to develop a novel algorithm other than viscose damping and mass-scaling.

As a start for the application of the DEM model, we have investigated two of the most important properties of fibre networks for hygiene products: ZD-compression and in-plane tensile properties. We have observed beautiful power-law relationships against density for compression stress and tensile strength. This may not be a complete coincidence, as the power-law relationships are reminiscent of percolation phenomena, and fibre networks in the low-to-medium density range are not far away from such percolation. In ZD-compression and in-plane tension cases, the low-energy deformation mode (bending) is the prevalent response. One important distinction of the compression behaviour is that the effects of the 3D nature of fibre properties, which are largely ignored in many network models, are very significant. This is because, for highly anisotropic fibre networks with very low (realistic) transverse fibre stiffness, the transverse compression can compete with or replace another low-energy deformation (bending).

One crucial point that would be an interesting direction for future work much suited for the models developed here is the role of fibre strength in the tensile strength of the fibre network. This has been a key topic almost since the inception of modern papermaking, and, as shown in the well-known Page's equation (Page, 1969), tensile strength of paper is believed to be controlled by fibre strength and bond strength. In this thesis, however, since the density range tested was focused on the low–medium range and since the single fibre strength values were mistakenly overestimated in this work resulting in no breakage of fibres, it was not possible to tackle this question.

References

Abd El-Rahman, A., & Tucker III, C. (2013). Mechanics of random discontinuous long-fiber thermoplastics. Part II: Direct simulation of uniaxial compression. *Journal of Rheology, 57*(5), 1463-1489.

Ban, E., Barocas, V., Shephard, M., & Picu, C. (2016). Softening in random networks of non-identical beams. *Journal of the Mechanics and Physics of Solids, 87*, 38-50.

Barbier, C., Dendievel, R., & Rodney, D. (2009). Role of friction in the mechanics of nonbonded fibrous materials. *Physical Review E, 80*(1).

Beil, N., & Roberts, W. (2002). Modeling and Computer Simulation of the Compressional Behavior of Fiber Assemblies: Part I: Comparison to van Wyk''s Theory. *Textile research journal, 72*(4), 341-351.

Beil, N., & Roberts, W. (2002). Modeling and computer simulation of the compressional behavior of fiber assemblies: part II: hysteresis, crimp, and orientation effects. *Textile research journal, 72*(5), 375-382.

Borodulina, S., Kulachenko, A., Galland, S., & Nygårds, M. (2012). Stress-strain curve of paper revisited. *Nordic Pulp and Paper Research Journal, 27*(2), 318-328.

Broedersz, C., & MacKintosh, F. (2014). Modeling semiflexible polymer networks. *Reviews of Modern Physics, 86*, 995.

Broedersz, C., Sheinman, M., & MacKintosh, F. (2012). Filament length controlled elasticity in 3D fiber networks. *Physical Review Letters, 108*, 078102–078106.

Campbell, J. (1963). Structural interpretation of paper elasticity. *Appita, 5*(16), 130-137.

Carnaby, G., & Pan, N. (1989). Theory of the compression hysteresis of fibrous assemblies. *Textile Research Journal, 59*(5), 275-284.

Cox, H. (1952). The elasticity and strength of paper and other fibrous materials. *British Journal of Applied Physics, 3*(3).

Cundall, P., & Strack, O. (1979). A discrete numerical model for granular assemblies. *Geotechnique, 29*(1), 47-65.

Durville, D. (2005). Numerical simulation of entangled materials mechanical properties. *Journal of materials science, 40*(22), 5941-5948.

Eriksson, M., Torgnysdotter, A., & Wågberg, L. (2006). Surface Modification of Wood Fibers Using the Polyelectrolyte Multilayer

Technique: Effects on Fiber Joint and Paper Strength Properties. *45*, 5279-5286.

Gurnagul, N., & Seth, R. (1997). Wet-web strength of hardwood kraft pulps. *Pulp and Paper Canada Ontario*(9), 305-309.

Hamlen, R. (1991). Paper structure, mechanics, and permeability: Computer-aided modeling. *Ph.D. thesis, University of Minnesota, USA*.

Head, D., Levine, A., & MacKintosh, F. (2003). Distinct regimes of elastic response and deformation modes of cross-linked cytoskeletal and semiflexible polymer networks. *Physical Review E, 68*, 061907.

Heyden, S. (2000). Network modelling for evaluation of mechanical properties of cellulose fibre fluff. *PhD Thesis, Lund University*.

Jangmalm, A. (1996). Network modelling of the elastic properties of paper. *Licentiate thesis, Dep. of Solid Mechanics, Royal Institute of Technology, Stockholm, Sweden*.

Kallmes, O., & Perez, M. (1965). A new theory for the load/elongation properties of paper. *Trans. Brit. Paper and Board Makers' Assoc. Sympos. Consol. Paper Web*, 779-800.

Kallmes, O., Stockel, I., & Bernier, G. (1963). The Elastic Behaviour of Paper. *Pulp Pap. Mag. Can., 64*(10), 449-456.

Komori, T., & Itoh, M. (1994). A modified theory of fiber contact in general fiber assemblies. *Textile research journal, 64*(9), 519-528.

Komori, T., & Makishima, K. (1977). Numbers of fiber-to-fiber contacts in general fiber assemblies. *Textile Research Journal, 47*(1), 13-17.

Komori, T., Itoh, M., & Takaku, A. (1992). A model analysis of the compressibility of fiber assemblies. *Textile research journal, 62*(10), 567-574.

Kulachenko, A., & Uesaka, T. (2012). Direct simulations of fiber network deformation and failure. *Mechanics of Materials, 51*, 1-14.

Lee, D., & Carnaby, G. (1992). Compressional Energy of the Random Fiber Assembly: Part I: Theory. *Textile research journal, 62*(4), 185-191.

Lee, D., & Lee, J. (1985). Initial compressional behaviour of fibre assembly. *Objective Measurements: Application to Product Design and Process Control*, 613-622.

Licup, A., Sharma, A., & MacKintosh, F. (2016). Elastic regimes of sub-isostatic athermal fiber networks. *Physical Review E, 93*(1), 012407.

Munjiza, A. (2004). *The combined finite-discrete element method.* John Wiley & Sons.

Page, D. (1969). A Theory for the Tensile Strength of Paper. *Tappi, 52*(4), 674-681.

Page, D., Seth, R., & De Grace, J. (1979). The elastic modulus of paper. *Tappi, 62*(9), 99-102.

Pan, N. (1993). A modified analysis of the microstructural characteristics of general fiber assemblies. *Textile Research Journal, 63*(6), 336-345.

Persson, J., & Isaksson, P. (2014). A mechanical particle model for analyzing rapid deformations and fracture in 3D fiber materials. *International Journal of Solids and Structures, 51*, 2244-2251.

Picu, R. (2011). Mechanics of random fiber networks - a review. *Soft Matter*(7), 6768-6785.

Qi, D. (1997). Microstructural model for a three-dimensional fiber network. *Tappi, 80*(1), 283-292.

Qi, D. (1997). Three-dimensional generalized anisotropic Cox-type structural model of a fiber network. *Tappi, 80*(11), 165-171.

Rigdahl, M., & Hollmark, H. (1986). *Paper structure and properties.* (J. Bristow, P. Koleth, & M. Dekker, Edits.)

Rigdahl, M., Westerlind, B., & Hollmark, H. (1984). Analysis of cellulose networks by the finite element method. *Journal of Materials Science, 19*, 3945-3952.

Rodney, D., Fivel, M., & Dendievel, R. (2005). Discrete modeling of the mechanics of entangled materials. *Physical review letters, 95*(10).

Räisänen, V., Alava, M., Nieminen, R., & Niskanen, K. (1996). Elastic-plastic behaviour in fibre networks. *Nordic Pulp and Paper Research Journal, 11*(4), 243-248.

Subramanian, G., & Picu, C. (2011). Mechanics of three-dimensional, nonbonded random fiber networks. *Physical Review E, 83*(5).

Toll, S. (1998). Packing mechanics of fiber reinforcements. *Polymer Engineering & Science, 38*(8), 1337-1350.

Toll, S., & Månson, J. (1995). Elastic Compression of a Fiber Network. *Journal of Applied Mechanics, 62*, 223-226.

Van den Akker, J. (1962). Some theoretical considerations on the mechanical properties. *Trans. Brit. Paper and Board Makers' Assoc. Sympos. Consol. Paper Web*, 205-241.

van Wyk, C. (1946). Note on the compressibility of wool. *Journal of the Textile Institute Transactions, 37*(12), 285-292.

Wang, Y. (2009). A new algorithm to model the dynamics of 3-D bonded rigid bodies with rotations. *Acta Geotechnica, 4*, 117-127.

Weatherley, D., Boros, V., & Hancock, W. (2014). ESyS-Particle Tutorial and User's Guide Version 2.3.1, 2014. *Earth Systems Science Computational Centre, The University of Queensland*.

Welling, U., & Germano, G. (2011). Efficiency of linked cell algorithms. *Computer Physics Communications, 182*(3), 611-615.

Wilhelm, J., & Frey, E. (2003). Elasticity of Stiff Polymer Networks. *Physical Review Letters, 91*, 108103.

Williams, J., & O'Connor, R. (1999). Discrete element simulation and the contact problem. *Archives of Computational Methods in Engineering, 6*(4), 279-304.

Yang, C. (1975). Plane modeling and analysis of fiber system. *Ph.D. thesis, University of Washington, USA.*

Zhu, H., Zhou, Z., Yang, R., & Yu, A. (2008). Discrete particle simulation of particulate systems: a review of major applications and findings. *Chemical Engineering Science, 63*(23), 5728-5770.

Åström, J., & Niskanen, K. (1991). Simulation of network fracture. *Proceedings of the 1991 International Paper Physics Conference, TAPPI.*

Åström, J., & Niskanen, K. (1993). Symmetry-Breaking Fracture in Random Fibre Networks. *Europhys. Lett., 21*(5), 557-562.

Åström, J., Saarinen, S., Niskanen, K., & Kurkijrvi, J. (1994). Microscopic mechanics of fibre networks. *Journal of Applied Physics, 75*(5), 2383-2392.